The Method of Lines Applied to a Finline/Strip Configuration on an Anisotropic Substrate

BRANDON M. SHERRILL, STUDENT MEMBER, IEEE, AND NICÓLAOS G. ALEXÓPOULOS, FELLOW, IEEE

Abstract—**The method of lines (MOL), a numerical scheme for the solution of partial differential equations that recently has been adapted to the full-wave dispersive characterization of planar waveguide structures, is modified to treat cases having uniaxially anisotropic dielectric regions. Anisotropy is present in commonly used substrate materials and typically leads to significant modeling error if neglected.**

The modus operandi of the method of lines is the discretization of spatial variables into a set of lines. Consequently, partial differential equations are reduced to ordinary kinds possessing simple, closed-form solutions. Being simple from the onset, the analysis effects an easily implemented method of good and controllable accuracy.

The paper's formulation is exercised upon an interesting form of finline, one with both a fin and an isolated strip opposite one another on a uniaxial substrate. Computations providing dispersive effective permittivities and impedances highlight the errors incurred in neglecting anisotropy.

I. Introduction

THE METHOD OF LINES (MOL), a general principle in the mathematical literature (e.g., Rothe [1], Faddeeva [2], Mikhlin *et al.* [3]), provides a simple means for characterizing the dispersive properties of transmission structures. The pioneering application of MOL to microwave theory by Schulz *et al.* [4]–[6] affords an accurate full-wave model of isotropic planar class waveguide structures (i.e., having plane dielectric regions separated by interface metallization). More recent formulations [7]–[11] exist to deal with special features such as nonuniform conductors and inhomogeneous or gyromagnetic regions. This paper reports an application of the basic method accounting for uniaxially anisotropic dielectrics. Anisotropy is present in commonly used substrate materials and usually produces significant modeling error if neglected [12]. Thus, the presented plan broadens the existing MOL literature to a wider class of materials (i.e., uniaxial).

MOL is a hybrid scheme incorporating components from both differential and difference analyses. Under it, all spatial variables but one of a scalar wave equation system are discretized. Upon a decoupling transformation, the system is solved exactly in closed form. No infinite summations [13], integrals [14], or basis functions [15] are present to impede calculation. Being simple from the onset, the analysis effects a method of good and controllable accuracy.

After exposition, this new formulation is exercised upon an interesting, relatively unstudied form of finline possessing both a fin and an isolated strip. Published results are available for this structure for isotropic substrates [6], [16], and comparisons of our results to these are excellent. After these checks, this paper proceeds to report on anisotropic cases, which deviate significantly from isotropic ones, lending import to its modeling.

II. Mathematical Formulation

General MOL principles are highlighted herein as the specific apparatus to treat the aforementioned finline is set up. The geometry considered is that of Fig. 1. This "fin-strip" is a uniform line possessing a fin of spacing s opposite a strip of width w on a dielectric substrate of thickness t. Conductors are assumed to be negligibly thin and lossless. The coupled version of this line (i.e., having dual strips) is found by Aikawa [17] to make possible directional coupler designs that were previously impractical. It is likewise the additional degree of freedom provided by its strip/slot combination that prompts study of this paper's structure. Also, Meier [18] reports that other advantages appear to be exhibited in general by such E-plane components. In the light of these notes, this waveguiding structure merits further attention.

The feature of interest is dielectric anisotropy. This paper assumes uniaxial regions with optical axes normal to region interfaces. Material is often supplied or selected in this orientation in attempts to suppress anisotropic behavior [19]. Hence, in the given coordinate system, each region possesses a tensor permittivity of the form ($\epsilon_{yy} = \epsilon_{\|}, \epsilon_{xx} = \epsilon_{zz} = \epsilon_{\perp}$):

$$\vec{\epsilon} = \epsilon_0 \begin{bmatrix} \epsilon_{\perp} & 0 & 0 \\ 0 & \epsilon_{\|} & 0 \\ 0 & 0 & \epsilon_{\perp} \end{bmatrix} \tag{1}$$

with relative permittivities $\epsilon_{\|}, \epsilon_{\perp}$ and free-space permittivity ϵ_0. Also, each region is assumed to be nonmagnetic with free-space permeability μ_0. As Fig. 1 indicates, the problem consists of three homogeneous regions (1,2,3). The central one is a dielectric described by $\epsilon_{\|}, \epsilon_{\perp} \neq 1$ while the two others are air.

Manuscript received November 7, 1986; revised January 31, 1987. This work was supported in part by the Northrop Corporation under a Northrop Fellowship in Electromagnetics.

The authors are with the Electrical Engineering Department, University of California, Los Angeles, CA 90024.

IEEE Log Number 8714114.

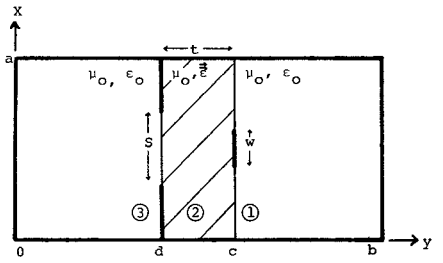

Fig. 1. Finline/strip configuration.

Having clarified the structure, determination of its fields is facilitated with Hertzian potentials having components in the optical axis direction [20]

$$\vec{\Pi}^{e,h} = \hat{y}\Pi^{e,h}(x, y, z). \tag{2}$$

Denoted by e, h, two potentials, the electric and the magnetic, comprise the modes forming the general hybrid solution. Assuming an $e^{+j\omega t}$ time-harmonic variation, the fields of a homogeneous region are

$$\vec{E}(x, y, z) = \nabla(\nabla\cdot\vec{\Pi}^e) + k_\perp^2\vec{\Pi}^e - j\omega\mu_0\nabla\times\vec{\Pi}^h \tag{3a}$$

and

$$\vec{H}(x, y, z) = j\omega\epsilon_0\epsilon_\perp\nabla\times\vec{\Pi}^e + \nabla(\nabla\cdot\vec{\Pi}^h) + k_\perp^2\vec{\Pi}^h \tag{3b}$$

where

$$k_\parallel = n_\parallel k_0, \quad k_\perp = n_\perp k_0, \quad k_0 = \omega\sqrt{\mu_0\epsilon_0} \tag{4a}$$

and

$$n_\parallel = \sqrt{\epsilon_\parallel}, \quad n_\perp = \sqrt{\epsilon_\perp}, \quad n = n_\parallel/n_\perp. \tag{4b}$$

Propagation in the $+z$ direction with phase constant β (to be determined) entails the functional dependence

$$\Pi^{e,h}(x, y, z) = \Psi^{e,h}(x, y)e^{-j\beta z}. \tag{5}$$

The transverse potentials $\Psi^{e,h}(x, y)$ are solutions to the scalar wave equations

$$\frac{\partial^2}{\partial x^2}\Psi^e(x, y) + n^2\frac{\partial^2}{\partial y^2}\Psi^e(x, y) + \left(k_\parallel^2 - \beta^2\right)\Psi^e(x, y) = 0 \tag{6a}$$

and

$$\frac{\partial^2}{\partial x^2}\Psi^h(x, y) + \frac{\partial^2}{\partial y^2}\Psi^h(x, y) + \left(k_\perp^2 - \beta^2\right)\Psi^h(x, y) = 0 \tag{6b}$$

for each region. This partial differential equation (PDE) set is the "input" to the method of lines. Through the "quantizing" of one of its independent variables, MOL approximates the PDE system to an ordinary differential equation (ODE) one yielding equations more readily solvable.

For this specific setup, the usual case of conductors placed symmetrically on the substrate is assumed. Taking this symmetry plane as a magnetic wall together with half a guide cross section yields an equivalent and more efficient problem still yielding the dominant mode. Now as

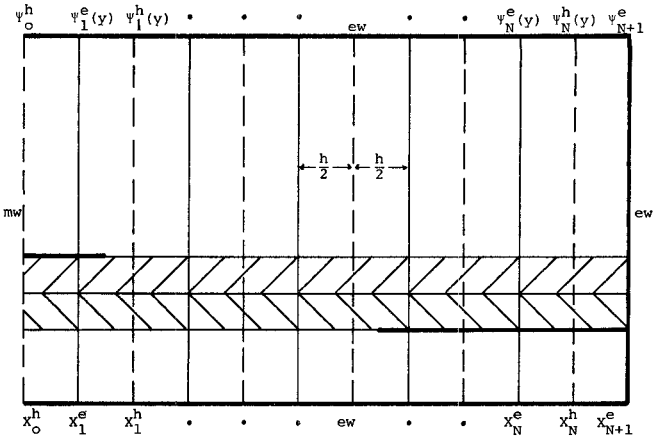

Fig. 2. Magnetic/electric sidewall discretization scheme.

the view of Fig. 2 shows, both potentials are sampled into the interior functions

$$\Psi_i^{e,h}(y) = \Psi^{e,h}\left(x_i^{e,h}, y\right), \qquad i = 1, \cdots, N \tag{7}$$

on N lines, each with spacing

$$h = \left(x_{N+1}^e - x_0^h\right)/(N + 1/2). \tag{8}$$

The magnetic and electric sidewalls are positioned respectively at x_0^h and x_{N+1}^e and are at the constant potentials Ψ_0^h and Ψ_{N+1}^e, respectively (both zero). Likewise, the scalar wave equations are discretized upon these lines, yielding for $i = 1, \cdots, N$

$$n^2\frac{d^2}{dy^2}\Psi_i^e(y) + \frac{1}{h^2}\left[\Psi_{i+1}^e(y) - 2\Psi_i^e(y) + \Psi_{i-1}^e(y)\right] + \left(k_\parallel^2 - \beta^2\right)\Psi_i^e(y) = 0 \tag{9a}$$

and

$$\frac{d^2}{dy^2}\Psi_i^h(y) + \frac{1}{h^2}\left[\Psi_{i+1}^h(y) - 2\Psi_i^h(y) + \Psi_{i-1}^h(y)\right] + \left(k_\perp^2 - \beta^2\right)\Psi_i^h(y) = 0. \tag{9b}$$

In this "discretized" domain, these are represented by

$$\bar{\Psi}^{e,h}(y) = \begin{bmatrix} \Psi_1^{e,h}(y) \\ \vdots \\ \Psi_N^{e,h}(y) \end{bmatrix} \tag{10}$$

and

$$n^2h^2\frac{d^2}{dy^2}\bar{\Psi}^e(y) - \left[\bar{\bar{D}}^e - h^2\left(k_\parallel^2 - \beta^2\right)\bar{\bar{I}}\right]\bar{\Psi}^e(y) = \bar{0} \tag{11a}$$

$$h^2\frac{d^2}{dy^2}\bar{\Psi}^h(y) - \left[\bar{\bar{D}}^h - h^2\left(k_\perp^2 - \beta^2\right)\bar{\bar{I}}\right]\bar{\Psi}^h(y) = \bar{0} \tag{11b}$$

where $\bar{\bar{I}}$ and $\bar{0}$ are the identity and null entities, respectively, and $\bar{\bar{D}}^{e,h}$ are the derivative matrices

$$\bar{\bar{D}}^{e,h} = \begin{bmatrix} D_1^{e,h} & -1 & & 0 \\ -1 & 2 & \ddots & \\ & \ddots & 2 & -1 \\ 0 & & -1 & D_2^{e,h} \end{bmatrix}_{N,N}. \tag{12}$$

The sidewall constants $D_1^{e,h}, D_2^{e,h}$ are from the set $\{1,2\}$ with $D_1^e = D_2^h = 1$, $D_2^e = D_1^h = 2$ for this discourse.

Uncoupling of the governing ODE set is possible by a linear transformation upon the potentials. A simple one exists as a consequence of the uncomplicated wall boundary conditions (i.e., lossless) and the unsophisticated discretization scheme (i.e., equispaced). In these other cases, this transformation must be approached numerically [11], but here analytic expressions are available [6]. Table I in [6] lists this transformational matrix in its forms versus sidewall type. Applying it to the derivative matrices, whose nondiagonal nature is yielding the coupling, gives

$$\bar{\bar{T}}_{e,h}^{t}\,\bar{\bar{D}}^{e,h}\bar{\bar{T}}_{e,h} = \tilde{\tilde{\lambda}}^{e,h} \tag{13}$$

where $\tilde{\tilde{\lambda}}^{e,h}$ are the achieved diagonal matrices, and t indicates transposition. Here, $\bar{\bar{T}}_e, \tilde{\tilde{\lambda}}^e$ are entries of the third row of [6, table I] and $\bar{\bar{T}}_h, \tilde{\tilde{\lambda}}^h$ are those of the second. When in conjunction with (13) the transformed potentials

$$\tilde{\Phi}^{e,h}(y) = \bar{\bar{T}}_{e,h}^{t}\bar{\Psi}^{e,h}(y) \tag{14}$$

are defined, an uncoupled wave equation system results:

$$n^2h^2\frac{d^2}{dy^2}\tilde{\Phi}^e(y) - \tilde{\tilde{\kappa}}_e^2\tilde{\Phi}^e(y) = \tilde{0} \tag{15a}$$

and

$$h^2\frac{d^2}{dy^2}\tilde{\Phi}^h(y) - \tilde{\tilde{\kappa}}_h^2\tilde{\Phi}^h(y) = \tilde{0} \tag{15b}$$

where for each region

$$\tilde{\tilde{\kappa}}_e^2 = \left[\tilde{\tilde{\lambda}}^e - h^2\left(k_{\|}^2 - \beta^2\right)\tilde{\tilde{I}}\right] \tag{16a}$$

and

$$\tilde{\tilde{\kappa}}_h^2 = \left[\tilde{\tilde{\lambda}}^h - h^2\left(k_{\perp}^2 - \beta^2\right)\tilde{\tilde{I}}\right]. \tag{16b}$$

A valuable property of this "transformed" domain is that all matrices in it are diagonal and so behave as vectors. This permits matrix equation algebra to be performed element-by-element rather than by grand manipulation. Hence, solutions to (15) are simply ($i = 1, \ldots, N$)

$$\Phi_i^e(y) = A_i^e\cosh\left(\frac{\kappa_{ei}y}{nh}\right) + B_i^e\sinh\left(\frac{\kappa_{ei}y}{nh}\right),$$
$$\kappa_{ei} = \left(\tilde{\tilde{\kappa}}_e\right)_i = \left[\left(\tilde{\tilde{\kappa}}_e^2\right)_i\right]^{1/2} \tag{17a}$$

and

$$\Phi_i^h(y) = A_i^h\cosh\left(\frac{\kappa_{hi}y}{h}\right) + B_i^h\sinh\left(\frac{\kappa_{hi}y}{h}\right),$$
$$\kappa_{hi} = \left(\tilde{\tilde{\kappa}}_h\right)_i = \left[\left(\tilde{\tilde{\kappa}}_h^2\right)_i\right]^{1/2} \tag{17b}$$

where the potential coefficients $A_i^{e,h}, B_i^{e,h}$ are indirectly obtained upon application of boundary conditions.

As is well known, varying geometries shape field structure through the influence of boundaries. In MOL, the influence of sidewalls is accounted for in the selection of the transformation matrices. The top and bottom walls are described by the direct conditions $d\tilde{\Phi}^e/dy = \tilde{\Phi}^h = \tilde{0}$. And field continuity for any dielectric–dielectric interface is attended to by

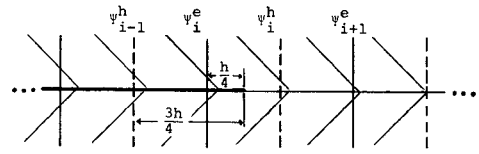

Fig. 3. Discretization with respect to an edge.

$$\frac{d\tilde{\Phi}_+^e}{dy} = \frac{d\tilde{\Phi}_-^e}{dy} \tag{18a}$$

$$\tilde{\Phi}_+^h = \tilde{\Phi}_-^h \tag{18b}$$

$$\omega\epsilon_0\beta\left(\epsilon_{\perp+}\tilde{\Phi}_+^e - \epsilon_{\perp-}\tilde{\Phi}_-^e\right) = \frac{1}{h}\tilde{\tilde{\delta}}\left(\frac{d\tilde{\Phi}_-^h}{dy} - \frac{d\tilde{\Phi}_+^h}{dy}\right) + \tilde{K}_z \tag{18c}$$

$$\frac{j\omega\epsilon_0}{h}\tilde{\tilde{\delta}}\left(\epsilon_{\perp+}\tilde{\Phi}_+^e - \epsilon_{\perp-}\tilde{\Phi}_-^e\right) = j\beta\left(\frac{d\tilde{\Phi}_+^h}{dy} - \frac{d\tilde{\Phi}_-^h}{dy}\right) + \tilde{K}_x \tag{18d}$$

where $\tilde{\tilde{\delta}}$ is the quantity in [6] and

$$\tilde{K}_x = \bar{\bar{T}}_h^t\bar{K}_x' \tag{19a}$$

$$\tilde{K}_z = \bar{\bar{T}}_e^t\bar{K}_z'. \tag{19b}$$

The terms $\bar{K}_{x,z}'$ are the constitutive sheet current densities (i.e., $K_{x,z}(x,z) = K_{x,z}'(x)e^{-j\beta z}$) discretized at points on the interface by the magnetic and electric potential lines, respectively.

Also, interface conductors, which make a structure interesting, influence the solution. They receive their attention later as a final boundary condition. Here, the discretization error caused by field/current singularities at their edges (the Meixner condition) is attended to. Schulz [21] finds this error to be negligible provided an edge exceeds its last intersecting Ψ^e line by $h/4$ and its last intersecting Ψ^h line by $3h/4$, as Fig. 3 clarifies. This rule has bearing on the choice of N. For a particular choice of physical dimensions, there exists an N set producing partitions nearly realizing this goal at each conductor edge. Stepping N member-by-member from this set enforces accuracy and monotonic convergence.

When these boundary conditions are tied together with the wave solutions, manipulation yields important interface equations. For this structure, the first is

$$\begin{bmatrix}\tilde{\Phi}_{2c}^e\\ \tilde{\Phi}_{2c}^h\\ \tilde{\Phi}_{2d}^e\\ \tilde{\Phi}_{2d}^h\end{bmatrix} = \left[\tilde{\tilde{Q}}\right]\begin{bmatrix}\tilde{K}_{zc}\\ \tilde{K}_{xc}\\ \tilde{K}_{zd}\\ \tilde{K}_{xd}\end{bmatrix} \tag{20}$$

where the subscripts c, d, and 2 indicate evaluation at

$y = c, d$ in region 2. Also arising is

$$\begin{bmatrix} \tilde{E}_{z2c} \\ \tilde{E}_{x2c} \\ \tilde{E}_{z2d} \\ \tilde{E}_{x2d} \end{bmatrix} = \left[\tilde{\tilde{P}}\right] \begin{bmatrix} \tilde{\Phi}^e_{2c} \\ \tilde{\Phi}^h_{2c} \\ \tilde{\Phi}^e_{2d} \\ \tilde{\Phi}^h_{2d} \end{bmatrix} \tag{21}$$

where

$$\tilde{E}_x = \bar{\bar{T}}_h^t \bar{E}'_x \tag{22a}$$

$$\tilde{E}_z = \bar{\bar{T}}_e^t \bar{E}'_z. \tag{22b}$$

The terms $\bar{E}'_{x,z}$ are the constitutive electric field intensities (i.e., $E_{x,z}(x, y, z) = E'_{x,z}(x, y)e^{-j\beta z}$) discretized at points on the interface by the magnetic and electric potential lines, respectively. Together, (20) and (21) state

$$\begin{bmatrix} \tilde{E}_{z2c} \\ \tilde{E}_{x2c} \\ \tilde{E}_{z2d} \\ \tilde{E}_{x2d} \end{bmatrix} = \left[\tilde{\tilde{Z}}\right] \begin{bmatrix} \tilde{K}_{zc} \\ \tilde{K}_{xc} \\ \tilde{K}_{zd} \\ \tilde{K}_{xd} \end{bmatrix}, \qquad \left[\tilde{\tilde{Z}}\right] = \left[\tilde{\tilde{P}}\right]\left[\tilde{\tilde{Q}}\right]. \tag{23}$$

As alluded to earlier, the final boundary conditions are those of the strip and slot. Enforcement relies upon the intersection of discretization lines with these features. Since small strips and slots are chosen for later computational examples, an economization is effected here in anticipation. Null tangential electric fields and null tangential sheet currents are imposed upon, respectively, the strip and slot, resulting in a reduced number of feature–potential line intersections (reducing computation). With this motive, (23) is reordered to

$$\begin{bmatrix} \tilde{E}_{z2c} \\ \tilde{E}_{x2c} \\ \tilde{K}_{zd} \\ \tilde{K}_{xd} \end{bmatrix} = \left[\tilde{\tilde{S}}\right] \begin{bmatrix} \tilde{K}_{zc} \\ \tilde{K}_{xc} \\ \tilde{E}_{z2d} \\ \tilde{E}_{x2d} \end{bmatrix}. \tag{24}$$

Upon the definition of a collective transformation matrix

$$\left[\bar{\bar{T}}\right] = \begin{bmatrix} \bar{\bar{T}}_e & \bar{\bar{0}} & \bar{\bar{0}} & \bar{\bar{0}} \\ \bar{\bar{0}} & \bar{\bar{T}}_h & \bar{\bar{0}} & \bar{\bar{0}} \\ \bar{\bar{0}} & \bar{\bar{0}} & \bar{\bar{T}}_e & \bar{\bar{0}} \\ \bar{\bar{0}} & \bar{\bar{0}} & \bar{\bar{0}} & \bar{\bar{T}}_h \end{bmatrix} \tag{25}$$

a final interface equation is possible in the discretized domain

$$\begin{bmatrix} \bar{E}'_{z2c} \\ \bar{E}'_{x2c} \\ \bar{K}'_{zd} \\ \bar{K}'_{xd} \end{bmatrix} = \left[\bar{\bar{S}}\right] \begin{bmatrix} \bar{K}'_{zc} \\ \bar{K}'_{xc} \\ \bar{E}'_{z2d} \\ \bar{E}'_{x2d} \end{bmatrix}, \qquad \left[\bar{\bar{S}}\right] = \left[\bar{\bar{T}}\right]\left[\tilde{\tilde{S}}\right]\left[\bar{\bar{T}}\right]^t. \tag{26}$$

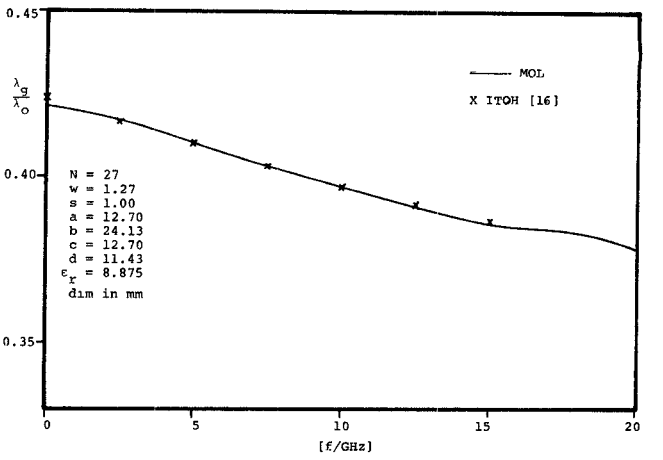

Fig. 4. Isotropic test case: guide wavelength.

Thus, the strip/slot boundary condition

$$\begin{bmatrix} \bar{E}'_{z2c} \\ \bar{E}'_{x2c} \\ \bar{K}'_{zd} \\ \bar{K}'_{xd} \end{bmatrix}_{\text{red}} = \bar{0} \tag{27}$$

at last implies the problem's dispersion equation:

$$\det\left[\bar{\bar{S}}(\omega, \beta)\right]_{\text{red}} = 0. \tag{28}$$

The subscript "red" stands for "reduced" and signifies inclusion only for matrix elements associated with potential lines intersecting the strip and slot. Thus, (28) yields, upon numerical solution, all phase constants of propagating modes at frequency f. Note that due to the isolated strip this structure always possesses an active mode (therefore, the dominant). With β now known, all guide fields are explicitly calculable, allowing further computations of interest to proceed (e.g., impedance). Lastly, it is the typically small order of the determinantal equation (28) that allows MOL to be accurate with small effort.

III. Computational Results

The method of lines developed in this paper enjoys very good agreement with other methods. Comparisons to isotropic shielded microstrip [22] and to anisotropic coplanar waveguide [23] show an average difference of 0.5 percent from these other theoretical calculations. This paper's structure also enjoys favorable comparisons. Itoh [16], using an immittance matrix approach, calculates for the isotropic case the dispersive normalized guide wavelength. With a moderate discretization ($N = 27$), MOL is within a 0.2 percent average difference of Itoh's example, as Fig. 4 illustrates. Itoh does not publish accompanying impedance figures, so a simple check is made with respect to the isotropic MOL formulation of Schulz *et al.* [6]. Fig. 5 presents the match between these dispersive impedance calculations (via strip current and guide power) under Itoh's parameters. With $N = 27$, agreement is within a 0.1-percent average difference. Collectively, these positive comparisons support this anisotropic MOL formulation.

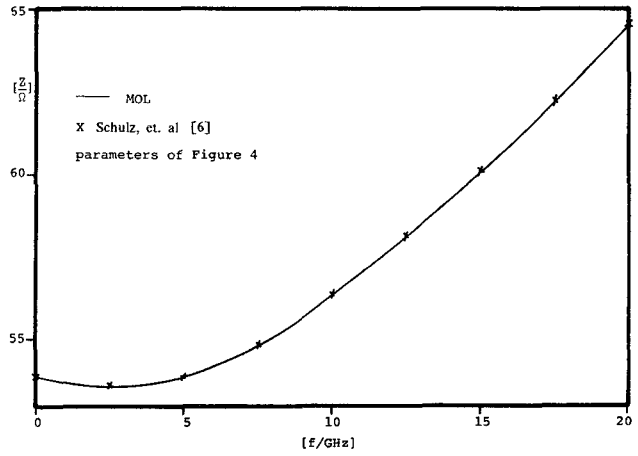

Fig. 5. Isotropic test case: impedance.

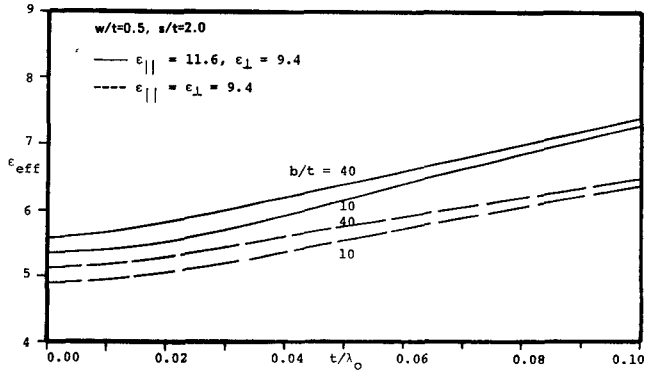

Fig. 6. Effective permittivity for a sapphire dielectric case.

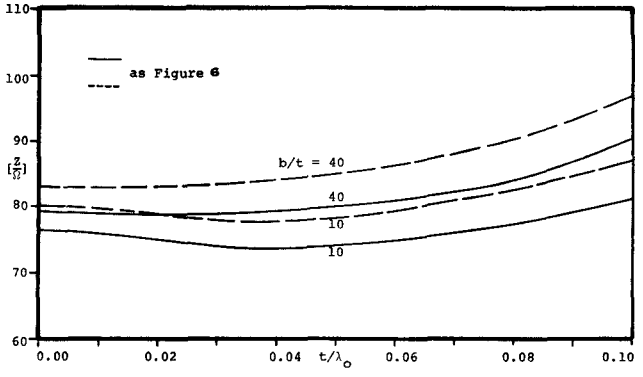

Fig. 7. Impedance for a sapphire dielectric case.

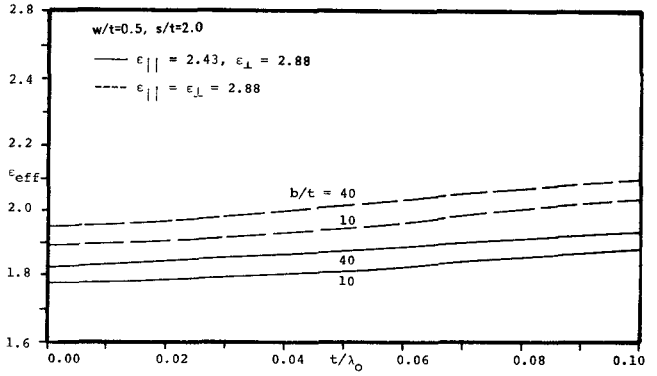

Fig. 8. Effective permittivity for a PTFE dielectric case.

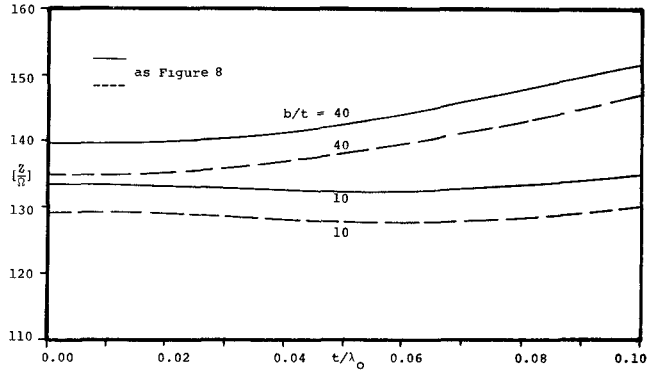

Fig. 9. Impedance for a PTFE dielectric case.

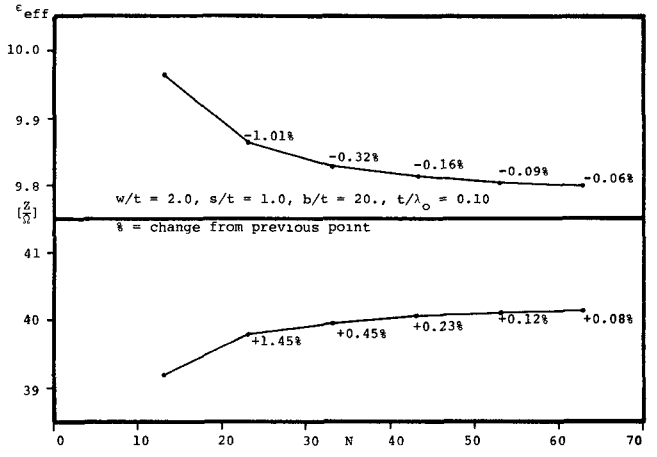

Fig. 10. Convergence behavior for a sapphire dielectric case.

Following are results from a larger study [24] exploring the "fin-strip" structure and the method's performance. Consider the issue of anisotropy brought up in Figs. 6–9. The curves are dominant-mode calculations to 0.5-percent accuracy for sapphire and PTFE examples relating effective permittivity ($\epsilon_{\text{eff}} = (\beta/k_0)^2$) and impedance (strip current-guide power) to the substrate thickness normalized to free-space wavelength. All numerical examples assume typical values for the strip/slot parameters and assume the usual choices of symmetrically placed conductors, a symmetrically placed slab, and a standard guide ($b/a = 2$). The first material, sapphire, is an attractively stable, high-permittivity substrate exhibiting a natural anisotropy of $\epsilon_{\|} = 11.6$, $\epsilon_{\perp} = 9.4$. Figs. 6 and 7 present curves observing these values and curves for the isotropic approximation $\epsilon_{\|} = \epsilon_{\perp} = 9.4$. This choice stems from the aforementioned approximation that in-plane permittivity controls [19]. However, it leads to errors in ϵ_{eff} of up to -11.6 percent and in Z of up to $+7.2$ percent for the range shown. The second material, PTFE, denotes a class of ceramic impregnated, low-permittivity Teflon substrates possessing manufacture-induced anisotropy. The member chosen here has the values [25] $\epsilon_{\|} = 2.43$, $\epsilon_{\perp} = 2.88$. Figs. 8 and 9 present curves for these and for the isotropic approxima-

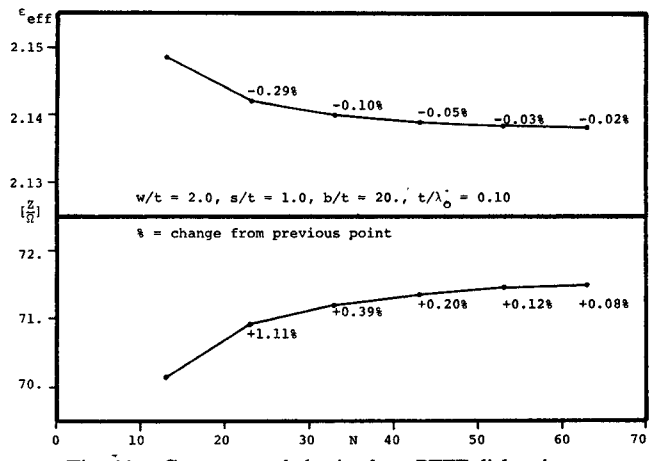

Fig. 11. Convergence behavior for a PTFE dielectric case.

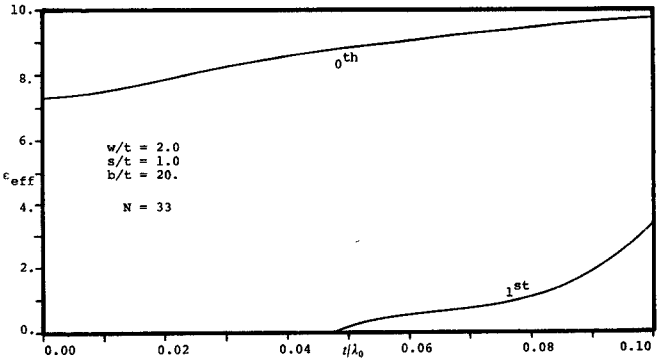

Fig. 12. First higher order mode for a sapphire dielectric case.

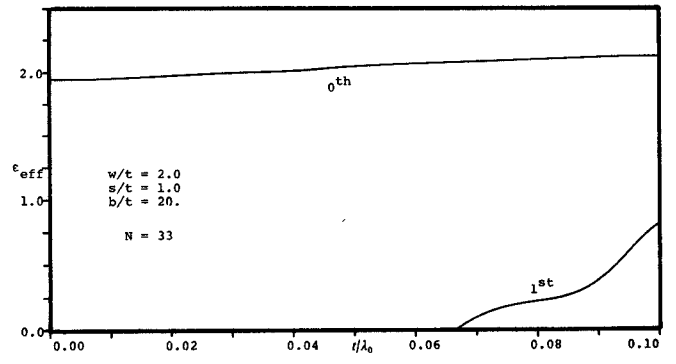

Fig. 13. First higher order mode for a PTFE dielectric case.

tion $\epsilon_{\|} = \epsilon_{\perp} = 2.88$. This approximation leads to errors in ϵ_{eff} of up to +8.8 percent and in Z of up to −3.6 percent for the range shown. A study of a number of cases [24] finds deviations from 1.6 percent to 18.4 percent. Work finds that no reasonable doctoring of an isotropic permittivity value will substitute satisfactorily for a material's anisotropic one. Compounding this inability with the observed errors lends weight to heeding anisotropy in modeling.

For MOL, N signifies the vector length of computational quantities and so is a measure of computational effort. Under the assumed parameters of Figs. 10 and 11, a search reveals the optimal N set (due to edge conditions) to be $\{13, 23, 33, \cdots\}$. These figures depict the (dominant-mode) convergence behavior of ϵ_{eff} and Z with respect to this set and illustrate the well-mannered convergence typical of MOL.

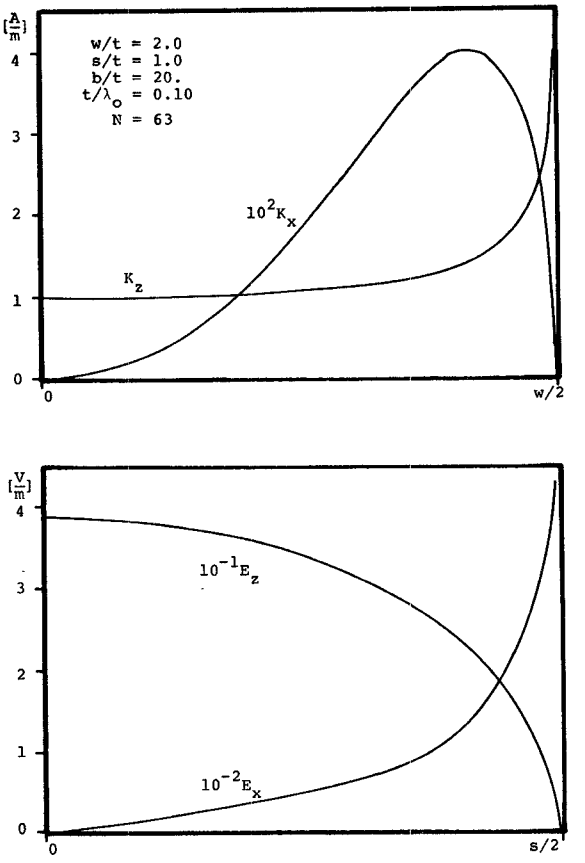

Fig. 14. Strip-currents/slot-fields for a sapphire dielectric case.

Of prime importance to single mode operation is knowledge of the next higher order one. Computations show it here also to occur for a central magnetic symmetry wall. For the assumed parameters, Figs. 12 and 13 show next higher order modes occurring at $t/\lambda_0 = 0.0477$ for sapphire and at $t/\lambda_0 = 0.0667$ for PTFE. When compared to ordinary waveguide of equal outside dimensions, one finds that the line delays higher mode turn-on (with lower permittivities aiding in this more).

For a particular choice of physical dimensions, the relative strip-current/slot-field distributions depend still upon frequency and mode number. It is instructive and interesting to view their shapes and relative magnitudes. Figs. 14 and 15 display typical dominant-mode, normalized values (at $N = 63$ for easy graphing). The computed currents follow a commonly observed shape [26], and the curves in all are consistent with the structure's boundaries. Relative to ordinary lines, this structure may experience lower losses overall. Computation shows that almost all guide power is confined to the substrate away from the large wall surfaces, which realistically impose some loss. However, admittedly, further calculations would have to be made to substantiate this.

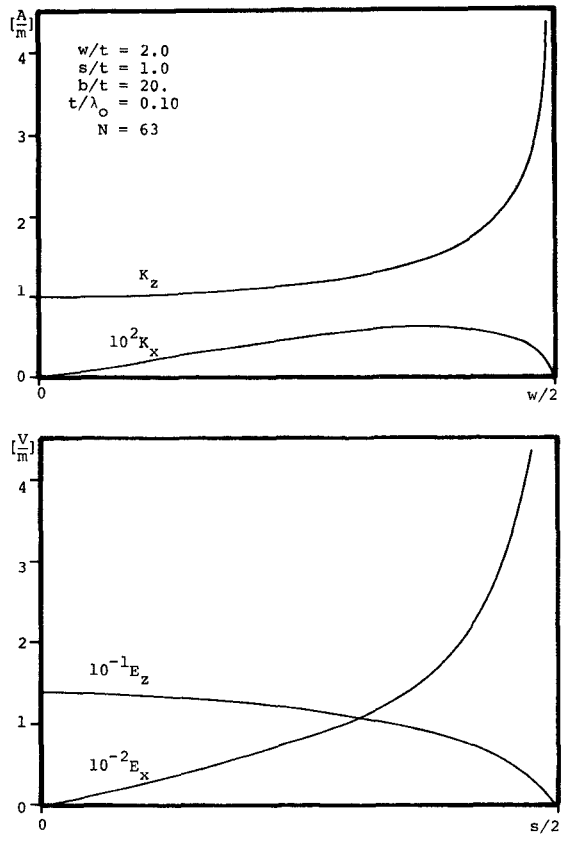

Fig. 15. Strip-currents/slot-fields for a PTFE dielectric case.

IV. Conclusions

The method of lines has been modified to deal with planar class waveguide problems having uniaxially anisotropic substrates. It was shown to be an accurate and simple full-wave scheme devoid of infinite summations, integrals, and basis functions. Application was made to a unique form of finline possessing both a strip and a slot for which dispersive effective dielectric constants and impedances were calculated. These characteristic values made obvious the errors incurred in neglecting anisotropy. Other associated results were discussed; among them was the good convergence behavior of MOL.

References

[1] E. Rothe, "Zweidimensionale Parabolische Randwertaufgaben als Grenzfall Eindimensionaler Randwertaufgaben," *Math. Ann.*, vol. 102, pp. 650–670, Mar. 1930.

[2] V. Faddeeva, "An approximate method of lines applied to certain boundary value problems," *Tr. Inst. Mat. Mek. Sverd.*, vol. 28, pp. 73–103, Feb. 1949.

[3] S. Mikhlin and K. Smolitskiy, *Naherungsmetoden zur Losung von Differential und Integralgleichungen*. Leipzig: Teubner-Verlag, 1969, pp. 238–244.

[4] U. Schulz, "Die Methode der Geraden—ein neus Verfahren zur Berechnung Plananer Mikrowellenstrukturen," Ph.D. dissertation, Fernuniversitaet Hagen, 1980.

[5] U. Schulz and R. Pregla, "A new technique for the analysis of the dispersion characteristics of planar waveguides," *Arch. Elek. Ubertragung.*, vol. 34, pp. 169–173, 1980.

[6] U. Schulz and R. Pregla, "A new technique for the analysis of the dispersion characteristics of planar waveguides and its application to microstrips with tuning septums," *Radio Sci.*, vol. 16, pp. 1173–1178, Nov.–Dec. 1981.

[7] S. Worm and R. Pregla, "Hybrid-mode analysis of arbitrarily shaped planar microwave structures by the method of lines," *IEEE Trans. Microwave Theory Tech.*, vol. MTT-32, pp. 191–196, Feb. 1984.

[8] R. Pregla and S. Worm, "A new technique for the analysis of planar waveguides with magnetized ferrite substrates," in *Proc. 12th European Microwave Conf.* (Helsinki, Finland), 1982, pp. 747–752.

[9] R. Pregla and S. Worm, "The method of lines for the analysis of planar waveguides with magnetized ferrite substrates," in *IEEE MTT-S 1984 Int. Microwave Symp. Dig.*, May 1984, pp. 348–350.

[10] H. Diestel, "Ein Verfahren zur Berechnung Planarer Dielektrischer Wellenleiter mit Ortsabhangiger Permittivitaet," Ph.D. dissertation, Fernuniversitaet Hagen, 1984.

[11] H. Diestel and S. Worm, "Analysis of hybrid field problems by the method of lines with nonequidistant discretization," *IEEE Trans. Microwave Theory Tech.*, vol. MTT-32, pp. 633–638, June 1984.

[12] N. G. Alexópoulos, "Integrated-circuit structures on Anisotropic substrates," *IEEE Trans. Microwave Theory Tech.*, vol. MTT-33, pp. 847–881, Oct. 1985.

[13] H. Hofmann, "Dispersion of planar waveguides for millimeter-wave application," *Arch. Elek. Übertragung*, vol. 31, pp. 40–44, 1977.

[14] E. Yamashita and K. Atsuki, "Analysis of microstrip-like transmission lines by nonuniform discretization of integral equations," *IEEE Trans. Microwave Theory Tech.*, vol. MTT-24, pp. 195–200, Apr. 1976.

[15] J. Knorr and P. Shayda, "Millimeter-wave fin-line characteristics," *IEEE Trans. Microwave Theory Tech.*, vol. MTT-28, pp. 737–743, July 1980.

[16] T. Itoh, "Spectral domain immittance approach for dispersion characteristics of shielded microstrips with tuning septums," in *Proc. 9th European Microwave Conf.* (Brighton, England), 1979, pp. 435–439.

[17] M. Aikawa, "Microstrip line directional coupler with tight coupling and high directivity," *Elect. and Comm. in Japan*, vol. J60-B, pp. 253–255, Apr. 1977.

[18] P. Meier, "Integrated fin-line millimeter components," *IEEE Trans. Microwave Theory Tech.*, vol. MTT-22, pp. 1209–1216, Dec. 1974.

[19] K. Gupta, R. Garg, and I. Bahl, *Microstrip Lines and Slotlines*. Dedham, MA: Artech House, 1979, p. 83.

[20] R. Collin, *Field Theory of Guided Waves*. New York: McGraw-Hill, 1960, pp. 101–102.

[21] U. Schulz, "On the edge condition with the method of lines in planar waveguides," *Arch. Elek. Übertragung*, vol. 34, pp. 176–178, 1980.

[22] G. Kowalski and R. Pregla, "Dispersion characteristics of shielded microstrips with finite thicknesses," *Arch. Elek. Übertragung*, vol. 25, pp. 193–196, 1971.

[23] A. Nakatani and N. G. Alexópoulos, "Toward a generalized algorithm for the modeling of the dispersive properties of integrated circuit structures on anisotropic substrates," *IEEE Trans. Microwave Theory Tech.*, vol. MTT-33, pp. 1436–1441, Dec. 1985.

[24] B. M. Sherrill, "The method of lines applied to a fin-line with an anisotropic substrate," M.S.E.E. thesis, Univ. of California, Los Angeles, 1986, pp. 37–67.

[25] M. Olyphant, Jr., "Measuring anisotropy in microwave substrates," in *IEEE MTT-S 1979 Int. Microwave Symp. Dig.*, Apr. 1979, pp. 91–94.

[26] M. Kobayashi, "Longitudinal and transverse current distributions on microstrip lines and their closed-form solution," *IEEE Trans. Microwave Theory Tech.*, vol. MTT-33, pp. 784–788, Sept. 1985.

✠

Brandon Mark Sherrill was born in Statesville, NC, on August 9, 1962. He received the B.S. degree (summa cum laude) in electrical engineer-

ing from North Carolina State University in 1984 and the M.S.E.E. degree from the University of California at Los Angeles in 1986.

He is currently working towards the Ph.D. degree at UCLA in modeling microwave and millimeter-wave devices and is an engineer at Northrop Corporation's Advanced Systems Division.

✠

Nicólaos G. Alexópoulos (S'68–M'69–SM'82) was born in Athens, Greece, in 1942. He graduated from the 8th Gymnasium of Athens

and subsequently obtained the B.S.E.E., M.S.E.E., and Ph.D. degrees from the University of Michigan, Ann Arbor, in 1964, 1967, and 1968, respectively.

He is currently a Professor in the Department of Electrical Engineering, University of California, Los Angeles, Associate Dean of the School of Engineering and Applied Science, and a Consultant with Northrop Corporation's Advanced Systems Division. His current research interests are in electromagnetic theory as it applies to the modeling of integrated-circuit components and printed circuit antennas for microwave and millimeter-wave applications, substrate materials and their effect on integrated-circuit structures and printed antennas, integrated-circuit antennas arrays, and antenna scattering studies. He is the Associate Editor of the IEEE TRANSACTIONS ON ANTENNAS AND PROPAGATION, *Electromagnetics Journal, and Alta Frequenza*.